The Role of the Residual Stresses of the Epoxy-Aluminum Interphase on the Interfacial Fracture Toughness

A. A. Roche
M. Aufray
Ingénierie des Matériaux Polymères/Laboratoire des Matériaux Macromoléculaires, Institut National des Sciences Appliquées de Lyon, Villeurbanne Cedex, France

J. Bouchet
Laboratoire de Technologie des Composites et Polymères, Ecole Polytechnique Fédérale de Lausanne, Lausanne, Switzerland

When an epoxy-diamine system (DGEBA-IPDA) is applied onto aluminum alloy (5754) and cured, an interphase having chemical, physical, and mechanical properties quite different from those of the bulk polymer is created between the substrate and the part of the polymer having bulk properties. To get a better understanding of the role of the interphase on the interfacial fracture toughness either a tri-layer (bulk coating/interphase/substrate) or a bi-layer model (bulk coating/substrate) were used for quantitative determination of the critical strain energy release rate (noted G_c). Indeed, as the interphase formation results from both dissolution and diffusion phenomena, we were able to control the interphase formation within coated systems by controlling the liquid-solid contact time and then to make tri- or bi-layered systems. The particularity of models used is to consider residual stress profiles developed within the entire system leading to an intrinsic parameter representing the work of adhesion between the polymer and the metallic substrate. The aim of this publication is to clearly establish the role of the interphase mechanical properties, such as Young's modulus and residual stress on the interfacial fracture toughness. Results are presented and discussed for three different aluminum surface treatments (chemical etching, degreasing and anodizing).

One of a Collection of papers honoring Hugh R. Brown, who received *The Adhesion Society Award for Excellence in Adhesion Science, Sponsored by 3M*, in February 2006. This paper is dedicated to the memory of Professor Alain Roche.

Address correspondence to Jérôme Bouchet, Laboratoire de Technologie des Composites et Polymères (LTC), Institut des Matériaux (IMX), MXG137, Station 12, Ecole Polytechnique Fédérale de Lausanne (EPFL), CH-1015 Lausanne, Switzerland. E-mail: jerome.bouchet@epfl.ch

Keywords: Fracture toughness; Interphase; Practical adhesion; Residual stresses; Work of adhesion

NOTATIONS

R_1	radius of curvature
ε^{ad}	adhesional strain
ε^{tot}	total strain
ε^{mech}	mechanical strain
x, y	coordinates
y_0	zero deformation
σ	residual stress
G_C	critical strain energy release rate
N	load
M	bending moment
E	Young's modulus
S	cross section (area)
δ	displacement
l	layer
W	energy
b	width
h	thickness
a	crack length
L	span length

The nth-order moment of a function f(y) is denoted: $\mu_n^f = \int_S f(y) y^n dS$ and $y_{0f} = \mu_1^f / \mu_0^f$

INTRODUCTION

Understanding the interphase is important for both fundamental and practical aspects of adhesion. Indeed the interphase and its properties determine the final overall properties of composite systems (practical adhesion, corrosion resistance, and durability) made of two components: the substrate and the polymer. Liquid epoxy-diamine mixtures are extensively used as adhesives or paints in many industrial applications. When they are applied onto metallic substrates and cured, epoxy-amine liquid monomers react with the metallic oxide and/or hydroxide to form chemical bonds [1] increasing practical adhesion (or adherence) between the epoxy polymer and the substrate surface [2,3]. Different studies report the influence of the nature of the

metallic substrate on the prepolymer cross-linking [4]. Unfortunately, only a few papers [5–8] have dealt with molecular structures formed within the interphase region. Moreover, when epoxy polymers are applied onto metallic substrates and cured, intrinsic and thermal residual stresses develop within the entire organic layer [9–11]. Intrinsic stresses are produced as a result of the mismatch between the active sites of the metallic substrate and the organic network and/or the formation of the polymer network. Thermal stresses are mostly developed during cooling [9–11] and are the result of thermal expansion mismatch between the metallic substrate and the polymer or cure-induced shrinkage of the organic layer [12]. Whatever their source, these residual stresses reduce the practical adhesion and may induce cracks in coating materials [13–15] resulting in a drop of the overall performance of adhesives or paints. To gain a better understanding of epoxy/metal adhesion requires a full knowledge of chemical and physical reactions which take place within the epoxy/metal interphase [16,17]. Thus, the polymer/substrate interphase is a complex region containing gradients of residual stresses and Young's modulus [18] resulting from structural rearrangement, intermolecular and inter-atomic interactions and diffusion phenomena [16]. When epoxy/metal systems fail, it is possible not only to correlate the residual stresses at the interphase/metal interface to practical adhesion but also to correlate the fundamental adhesion and durability to the presence or not of some chemical species [19]. Usually, when adhesional failure of the organic layer is observed, the practical adhesion is characterized by an appropriate yield criterion such as ultimate load (lap-shear, pull-out, and flexure tests [16,20,21]). Unfortunately, this kind of parameter is strongly dependent on the specimen geometry [16]. Therefore, a criterion based on the fracture energy rather than strength is more suitable for describing the practical adhesion [22,23]. To study the crack (or failure) propagation, the linear elastic fracture mechanics theory provides an energy criterion: the critical strain energy release rate, G_c, which represents the sum of all energy losses incurred around the crack tip and which is, therefore, the energy required to increase the crack by unit length in a specimen of unit width [24–27]. Thus, an adhesional failure is generally associated with mode-I (tensile) and/or mode-II (shear) fractures along the debonded interface.

OVERVIEW OF THE PRESENT WORK

In recent works we have determined several mechanisms of the epoxy/aluminum interphase formation leading to a better understanding of

its chemical, physical, and mechanical properties [28–31]. The organic layer near the substrate surface has to be considered as an interphase containing gradients of residual stresses and Young's modulus resulting from structural rearrangement, intermolecular and inter-atomic interactions, and diffusion phenomena, and where some new chemical species may be formed. In the following we consider the interphase as a third layer of the polymer/substrate system where mechanical, physical, and chemical properties are different from those of the bulk polymer. We called "bulk coating" that part of the coating having bulk properties. The aim of this article is to understand and establish the role of the interphase on the interfacial fracture toughness. As the interphase formation results from both dissolution and diffusion phenomena, we were able to control the interphase formation within coated systems by controlling the liquid-solid contact time and then to make tri- or bi-layered systems. So, we determined the critical strain energy release rate, G_c, using a model recently developed, based on a three-point flexure test [32–34]. The particularity of this model is to take into account both the mechanical properties such as the Young's modulus gradient and also residual stress profile within a bi- or tri-layered system. The advantage of using such a model is to have an intrinsic parameter representing the work of adhesion between the polymer and the metallic substrate.

EXPERIMENTAL

Materials

The metallic substrates used were either 0.500 ± 0.005 mm or 0.800 ± 0.005 mm thick 5754 commercial aluminum alloy from Péchiney, Voreppe, France. Aluminum sheets were prepared by die-cutting to provide identical sized strips ($150 \times 10\,mm^2$). Before any polymer application aluminum substrate surfaces were degreased, chemically etched or anodized as shown in Table 1.

After surface treatment all substrates were stored less than 2 hours in an air-conditioned room ($20 \pm 2^{\circ}C$ and $50 \pm 5\%$ RH). The epoxy prepolymer used was pure diglycidyl ether of bisphenol A (DGEBA, M.W. = 348 g/mol; DER 332 from Dow Chemical, Rheinmünster, Germany). The curing agent was isophorone-diamine (3-aminomethyl-3,5,5-trimethylcyclohexylamine) (IPDA from Fluka, Lausanne, Switzerland). All chemicals were used without further purification. The stoichiometric ratio (a/e, aminohydrogen/epoxy) used was equal to 1. This ratio was calculated using a functionality of 4 for the diamine and 2 for the epoxy monomer. Homogeneous mixtures of DGEBA and

TABLE 1 Surface Treatments of Aluminum Alloy (5754)

Treatment	Description
Degreasing	Ultrasonically cleaned in acetone for 10 min and wiped dry
Anodizing	Ultrasonically cleaned in acetone for 10 min, wiped dry, anodized at 10 V for 20 min in a 1 M phosphoric acid solution at 20°C, rinsed in running tap water for 1 min, allowed to stand in deionized water for 5 min and wiped dry
Chemical etching	Ultrasonically cleaned in acetone for 10 min, wiped dry, submerged in a 2% sulfuric acid solution (Ridoline 124, from Fischer-chemie, Aschaffenburg, Germany), at 60°C for 1 min 30 sec, rinsed in running tap water for 1 min, allowed to stand in deionized water for 5 min and wiped dry

IPDA were achieved by stirring in vacuum (≈1 Pa) at room temperature (Rotavapor RE 211 from BÜCHI, Flawil, Switzerland) for 30 minutes to avoid any air bubble formation. The epoxy-diamine mixture was applied to treated metallic sheets to obtain the desired coating thickness using an automatic film applicator (from Sheen, Middlesex, UK). The coating layer and substrate have the same widths for residual stresses and Young's modulus determinations.

For practical adhesion measurement using the three-point flexure test, the DGEBA-IPDA mixture was applied onto degreased, anodized or chemically etched aluminum by applying 0.5 ml with a syringe on each sample. The mould was made of RTV-501 (Rhone Poulenc, Lyon, France). The adhesive block formed had dimensions $25 \times 5 \times 4\,\text{mm}^3$ [35]. Either the ultimate load (F_{max}) or the ultimate displacement (d_{max}) were used to evaluate the practical adhesion of DGEBA-IPDA polymer on metallic substrates (see Figure 1).

Series of six samples were prepared. To determine the Young's modulus of the bulk organic materials cured, two $150 \times 10 \times 2\,\text{mm}^3$ bars were molded in a room temperature vulcanizing silicone (RTV) mold. To allow chemical reactions between the substrate surface and liquid monomers to take place, leading to full interphase formation, liquid monomers were kept in contact with the metallic surface for 3 hours at room temperature before starting the adhesive curing cycle [36]. The adhesive curing cycle, denoted (i), allowing the maximum conversion of the polymer and the maximum glass transition temperature ($T_g^\infty = 163°\text{C}$) was $20 \rightarrow 60°\text{C}$ at 2°C/min; 2 hours at 60°C; $60 \rightarrow 140°\text{C}$ at 2°C/min; 1 hour at 140°C; $140 \rightarrow 190°\text{C}$ at 2°C/min; 6 hours at 190°C; and cooling (8 hours) down to 20°C in the oven (see Figure 2).

Conversely, when we did not want the interphase formation, right after the epoxy-diamine application the coated specimens were placed

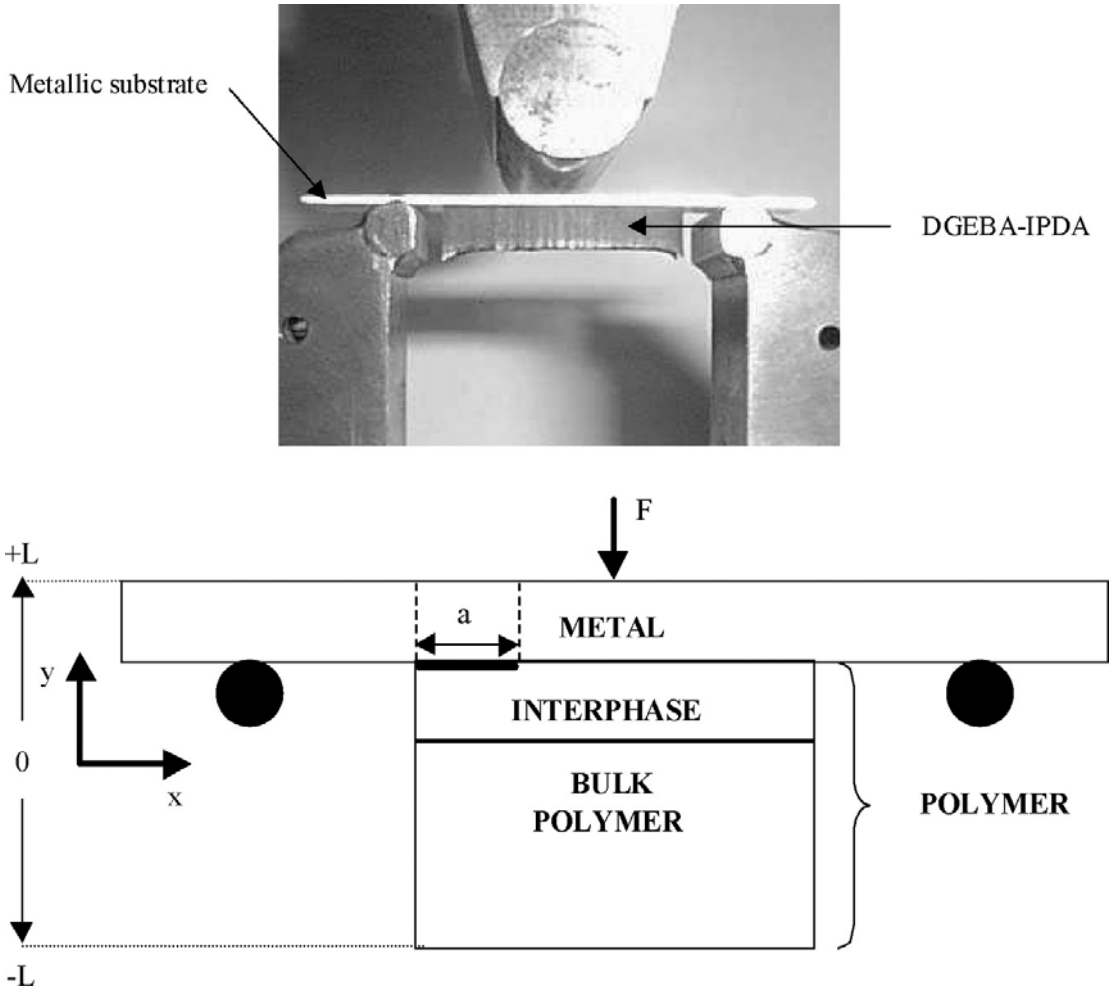

FIGURE 1 Three-point flexure test.

in a preheated oven at 190°C, held for 6 hours and cooled down to 20°C in the oven during 8 hours. This curing cycle is denoted (ii) (see Figure 2).

Infra-red Spectroscopy (μFTIR)

Micro-IR maps were made using an FTIR Imaging Spotlight 300 (from Perkin Elmer™, Courtaboeuf, France). To determine the practical adhesion, thick stiffeners ($25 \times 5 \times 4\,mm^3$) made of polymer were moulded onto the metallic substrate and debonded by mechanical testing with a three-point flexure test (ISO 14679). After this test, it was possible to cut 1 mm thick slices of polymer (perpendicularly to the adherent surface) and to analyze them. A transmission infrared map is realized by collecting data points every 6 μm using a sample displacement stage along a line perpendicular to the metal surface.

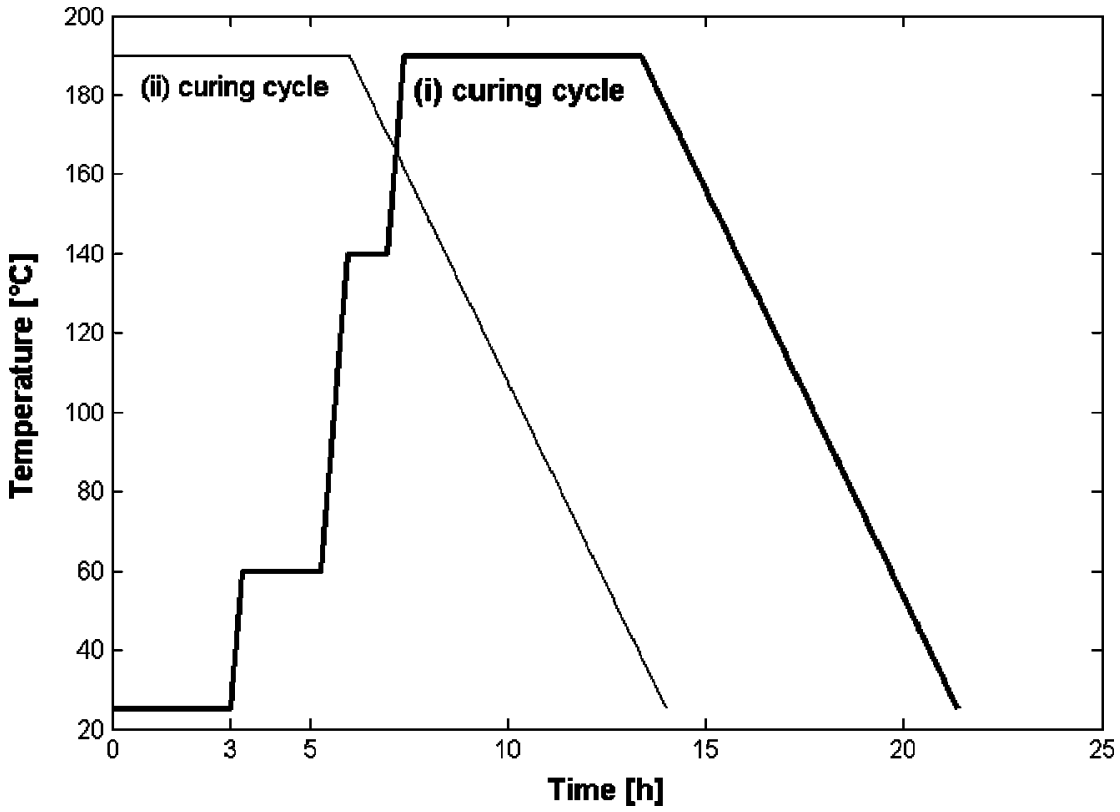

FIGURE 2 (i) and (ii) curing cycles.

According to the D66545 Perkin Elmer Product Note, the dual imaging resolution was 6.25 μm pixel size. Infrared spectra were recorded in the 3000–7800 cm^{-1} range using a Dual mode Detector. Imaging mode was used. For each analysis 16 scans were collected at 16 cm^{-1} resolution. We measured the 6500 cm^{-1} amine band with the 4623 cm^{-1} aromatic C−H ring stretch combination band used as reference. Normalized amine band intensity variations are derived from μ-IR spectroscopy for DGEBA/IPDA.

Young's Modulus of Thin Films

This work was performed with a three-point flexure machine (FLEX3, Techmétal, Maizières-les-Metz, France) [37,38]. The crosshead displacement speed was 0.1 mm/min. A 50 N full scale load cell with a sensitivity of ± 5 mN and a stiffness of 2.2×10^5 N/mm was fitted under the crosshead. The load (P) *versus* displacement (δ) curves (P/δ curves) were recorded. The slopes of the P/δ curves, within the linear region, were then computed using a linear regression program. Experimental curve slopes were corrected to take into account the load cell stiffness as described previously [35]. For various spans

(L_j), the apparent modulus $(E_{app})_j$ can be calculated from the slope $(P/\delta)_j$ of the load-displacement curve. The extrapolated Young's moduli of the substrate and the entire coated system can be obtained from curves of (E_{app}) as a function of (h/L_j). It has been reported that the extrapolated Young's modulus is independent of the width/thickness ratio, and, thus, the transverse effect (Poisson's ratio) will not be considered [39].

Radius of Curvature Determination

Experiments were carried out with a flexure machine (FLEX3, Techmétal, Maizières-les-Metz, France) equipped with a 50 N full-scale load cell with a sensitivity of ± 5 mN and a stiffness of 2.2×10^5 N/mm. Coated samples were placed on a planar and rigid material. Assuming that the radius of curvature is large compared with both the length and the thickness of the multilayer beam, it can be considered that the length of the neutral axis is equal to its span. For such a curved multi-layer beam of neutral axis length (L in mm) and maximal deflection (δ_{max} in mm) at the mid-span (L/2) the radius of curvature is given by:

$$R_1 = \frac{L^2}{8\delta_{max}} \tag{1}$$

Residual Stress Calculation

In previous works [28–31] we have shown that an interphase thickness in a range of 200–300 μm was formed for the DGEBA-IPDA/aluminum system. A profile of residual stresses within the tri-layer system (bulk coating/interphase/substrate) was also reported [32]. During the curing cycle each material forming the tri-layer system is subject to strains, which can be either of chemical and/or thermal origin. We have called them adhesional strains [33]. The model developed to determine the profile of residual stresses was based on the identification of adhesional strains. Using the measured radius of curvature it was possible to calculate the resulting mechanical strain in order to obtain the stress in each material. Thus, we have assumed that the total strain in the tri-layer system is:

$$\varepsilon^{tot}(y) = \varepsilon^{mech}(y) + \varepsilon^{ad}(y) = \frac{y - y_0}{R_1} \tag{2}$$

In the longitudinal direction, the final uni-axial residual stresses of the tri-layer system (bulk coating/interphase/substrate) are given by:

$$\sigma = E(y)\left[\frac{y - y_0}{R_1} - \varepsilon^{ad}(y)\right] \tag{3}$$

y_0 and R_1 are obtained as (see Reference [29] for more details):

$$R_1 = -\frac{\mu_2^E \mu_0^E - (\mu_1^E)^2}{\mu_0^{\varepsilon^{ad}E}\mu_1^E - \mu_0^E \mu_1^{\varepsilon^{ad}E}} \qquad \text{and} \qquad y_0 = \frac{\mu_2^E - y_{0\varepsilon^{ad}E}\mu_1^E}{\mu_1^E - y_{0\varepsilon^{ad}E}\mu_0^E} \tag{4}$$

It is possible to determine the adhesional strain evolution law by using the radius of curvature. To identify the adhesional strains, a knowledge of Young's modulus as a function of the position within the interphase is necessary. Figure 3 represents the variation of the Young's modulus within the entire tri-layer system for degreased, chemically etched and anodized aluminum substrates in the case of a tri-layer system (curing cycle [i]). The Young's modulus decreases within the interphase as a function of the coating thickness and remains constant for films thicker than 0.2 mm (*i.e.*, for the part of the coating having the bulk properties). From the Young's modulus values obtained in Figure 3 the interphase was discretized into 3 linear regions v of

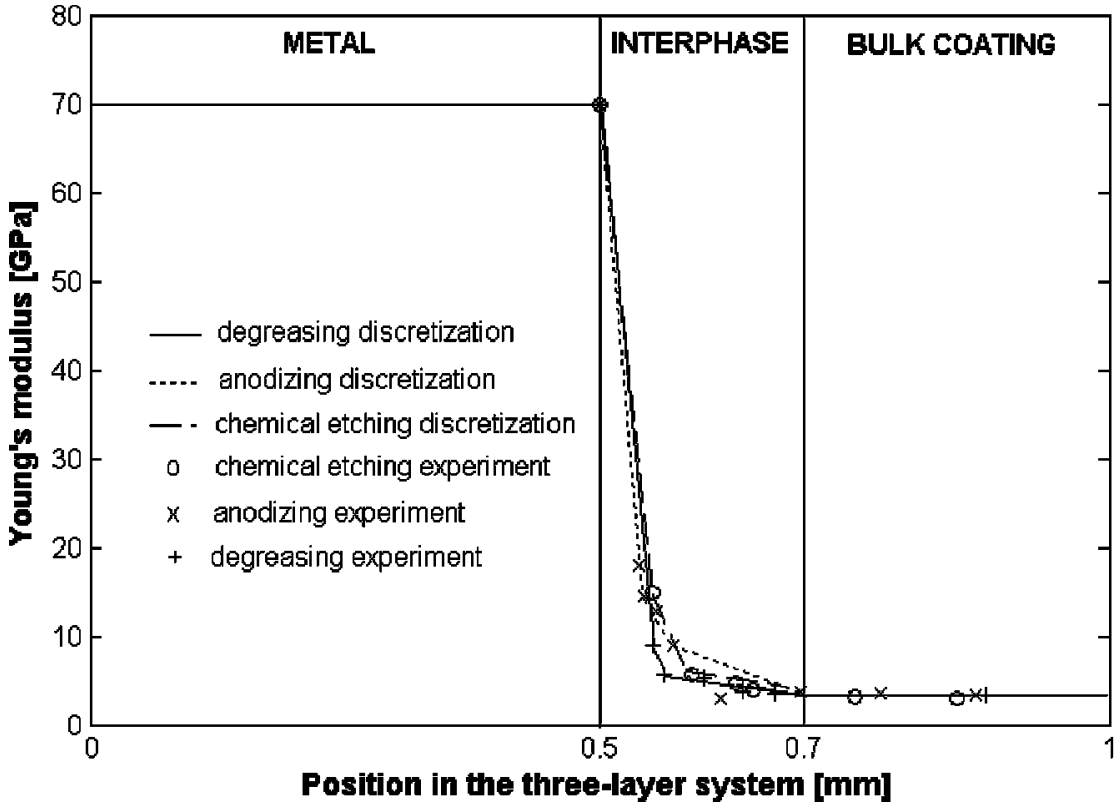

FIGURE 3 Variation of the Young's modulus as a function of the position in the three-layer system.

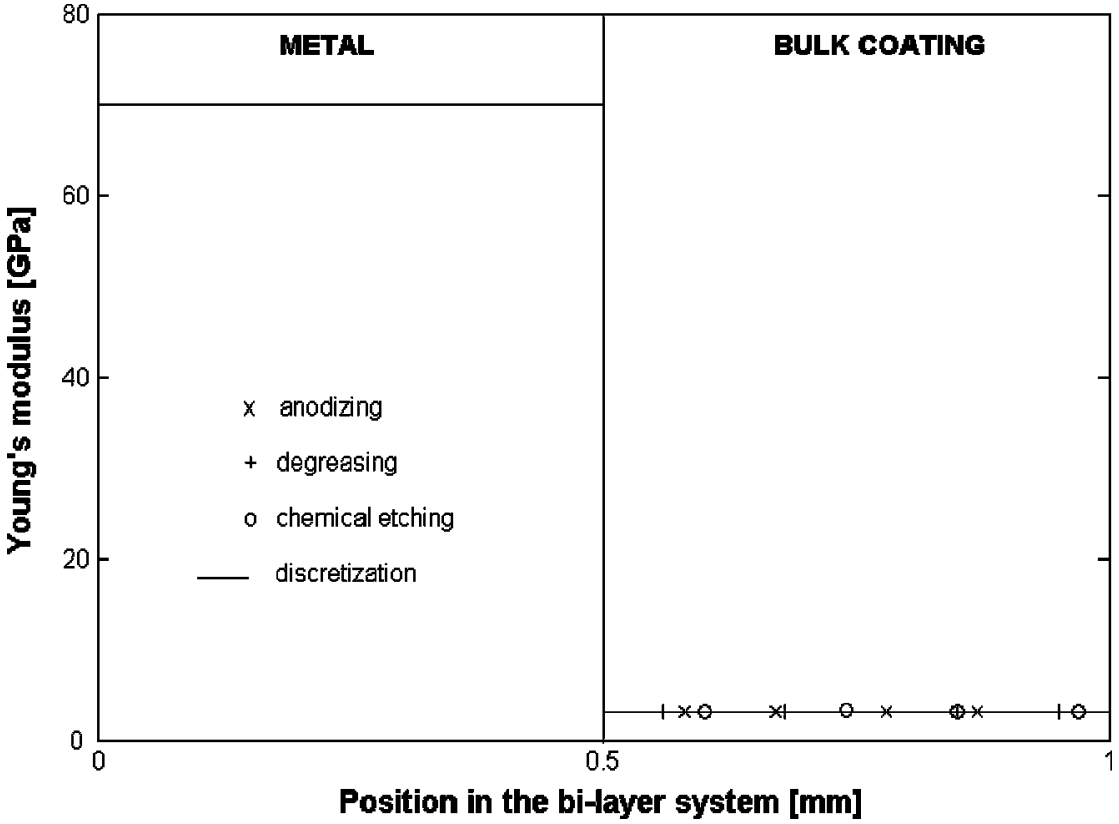

FIGURE 4 Variation of the Young's modulus as a function of the position in the bilayer system.

thickness *dhv*, irrespective of metallic surface treatment. At the interphase/metal interface Young's modulus of the aluminum substrate (*i.e.*, 70 GPa) was taken and at the bulk coating/interphase interface we have taken Young's modulus of the bulk coating (*i.e.*, 3.2 GPa). The adhesional strains within the interphase were considered linear and continuous and as constant within both metal and bulk as mentioned previously [33]. When a bi-layer system is obtained (curing cycle [ii]) the interphase thickness is considered as nil and the variation of the Young's modulus in such bi-layer system is represented in Figure 4.

Practical Adhesion Measurements

To determine the practical adhesion of coatings to metals Roche *et al.* [37] introduced a three point flexure sample geometry (see Figure 1). This three-point flexure test has already been extensively described [35,36] and standardized (ISO 14679–1997). This test was performed with a flexure machine (FLEX3, Techmétal, Maizières-les-Metz,

France) fitted with a 1000 N full-scale load cell with a sensitivity of ± 0.1 N and a stiffness of 1.1×10^7 N/mm, at a crosshead displacement speed of 0.5 mm/min. In a first approximation, the specimen can be analyzed using the classical beam theory. We assume a crack length (a) at the interface between the stiffener (*i.e.*, interphase + bulk coating) and the substrate (see Figure 1). The total strain within the tri-layer system (bulk coating/interphase/substrate) is expressed by:

$$\varepsilon_x^{tot}(x,y) = \varepsilon_x^{mech}(x,y) + \varepsilon^{adh}(y) = \frac{y - y_0(x)}{R_1(x)} \tag{5}$$

The values of R_1 and y_0 are determined by writing the two equilibrium conditions for the force and the moment for any cross section of the bulk coating/interphase/substrate system. The result is:

$$\begin{aligned} R_1(x) &= \frac{\mu_2^E \mu_0^E - (\mu_1^E)^2}{-\mu_0^{\varepsilon^{ad}E} \mu_1^E + \mu_0^E (\mu_1^{\varepsilon^{ad}E} + M(x))} \quad \text{and} \\ y_0(x) &= \frac{\mu_1^E (\mu_1^{\varepsilon^{ad}E} + M(x)) - \mu_2^E \mu_0^{\varepsilon^{ad}E}}{\mu_0^E (\mu_1^{\varepsilon^{ad}E} + M(x)) - \mu_1^E \mu_0^{\varepsilon^{ad}E}} \end{aligned} \tag{6}$$

When a bilayer model is desired, the interphase thickness in Equation (6) is considered as nil (*i.e.*, $h_i = 0$). When residual stresses are neglected, adhesional strains in Equation (6) are equal to zero (*i.e.*, $\varepsilon_m^{ad} = \varepsilon_i^{ad} = \varepsilon_{bc}^{ad} = 0$). Moreover, the experimental ultimate parameters F_{max} or d_{max} (*i.e.*, the ultimate load or ultimate displacement) are associated with a critical crack size inducing a significant variation of the sample stiffness. This point is generally associated with the initiation of fracture, because it corresponds to the minimum size of the experimental crack which can be mechanically detected before propagation of the fracture, using ultrasonic detection. In fact, at this ultimate point, the fracture has already been initiated, as previously reported [40]. So, we assumed that, at this point, the theory of linear fracture mechanics was applicable since this point corresponded to a crack length (a), tending to zero ($a \to 0$). When $a \to 0$, we can also assume that the beam theory assumptions are still valid. Because the failure propagation in our experiments was always nearly instantaneous Equation (7) can be written for constant displacement (δ). In previous work [30] using a finite element model the cracked three-point flexure test was analyzed and shown to yield predominantly mode I fracture. So, in first approximation: $G_c^{flexure} = G_{Ic}^{flexure}$. Thus, the critical energy release rate, in the case of the three-point flexure test, is given by the following equation (see Reference [33] for more details):

$$G_{Ic}^{flexure} = -\frac{1}{b}\left[\frac{\partial}{\partial a}\left[\int_0^L \left(\int_{S(x)} \frac{1}{2}E(x,y)\left[\frac{y-y_0(x)}{R_1(x)} - \varepsilon^{ad}(y)\right]^2 dS\right)dx\right]\right]_{\delta} \quad (a \to 0) \tag{7}$$

RESULTS AND DISCUSSIONS

When liquid epoxy-diamine prepolymers were applied onto metallic substrates, interphases between the coating part having the bulk properties and the metallic surface were created. Chemical, physical, and mechanical properties of the formed interphase depend on both the substrate surface and the diamine hardener. In previous works we have pointed out that the interphase formation mechanisms result from dissolution and diffusion phenomena [28–30]. No chemical reaction was observed when the pure DGEBA monomer was applied onto the metallic surfaces or when pure diamine monomers were applied onto gold coated substrates. On the contrary, when pure diamine monomers were applied onto either titanium or aluminum metallic surfaces, chemical reactions occurred. Following chemical sorption of the amine onto oxidized or hydroxided metallic surfaces, a partial dissolution of the surface oxide (and/or hydroxide) was observed according to the basic behavior of diamine monomers. Then metallic ions diffuse within the liquid monomer mixture (epoxy-diamine) and react by coordination with amine groups of the diamine monomer to form organo-metallic complexes (or chelates). When the complex concentration is higher than its solubility limit, complexes (or chelates) crystallize as sharp needles. During the curing cycle, organo-metallic complexes react with the epoxy monomer leading a phase separation corresponding to the formation of a new epoxy network having a lower Tg. Moreover, crystals not dissolved after the curing cycle act as short fibers in the organic matrix, leading to an increase of the Young's modulus. The same mechanisms were observed for Sn, Zn, Fe, Cr, Cu, and Ti [28,41] metallic substrates covered by their oxide or hydroxide layer, and for E-glass substrate. Because dissolution and diffusion phenomena were expected, the interphase formation should be related to the liquid-solid contact duration between liquid prepolymers and metallic substrates. To illustrate this point we have plotted in Figure 5 the variation of the ultimate load (determined using a three-point flexure test), the relative absorbance of OH groups (determined using reflectance infrared spectroscopy at $3300\,cm^{-1}$), the glass transition temperature (determined using a 150-μm thick coating) and the Young's modulus (determined using a three-point

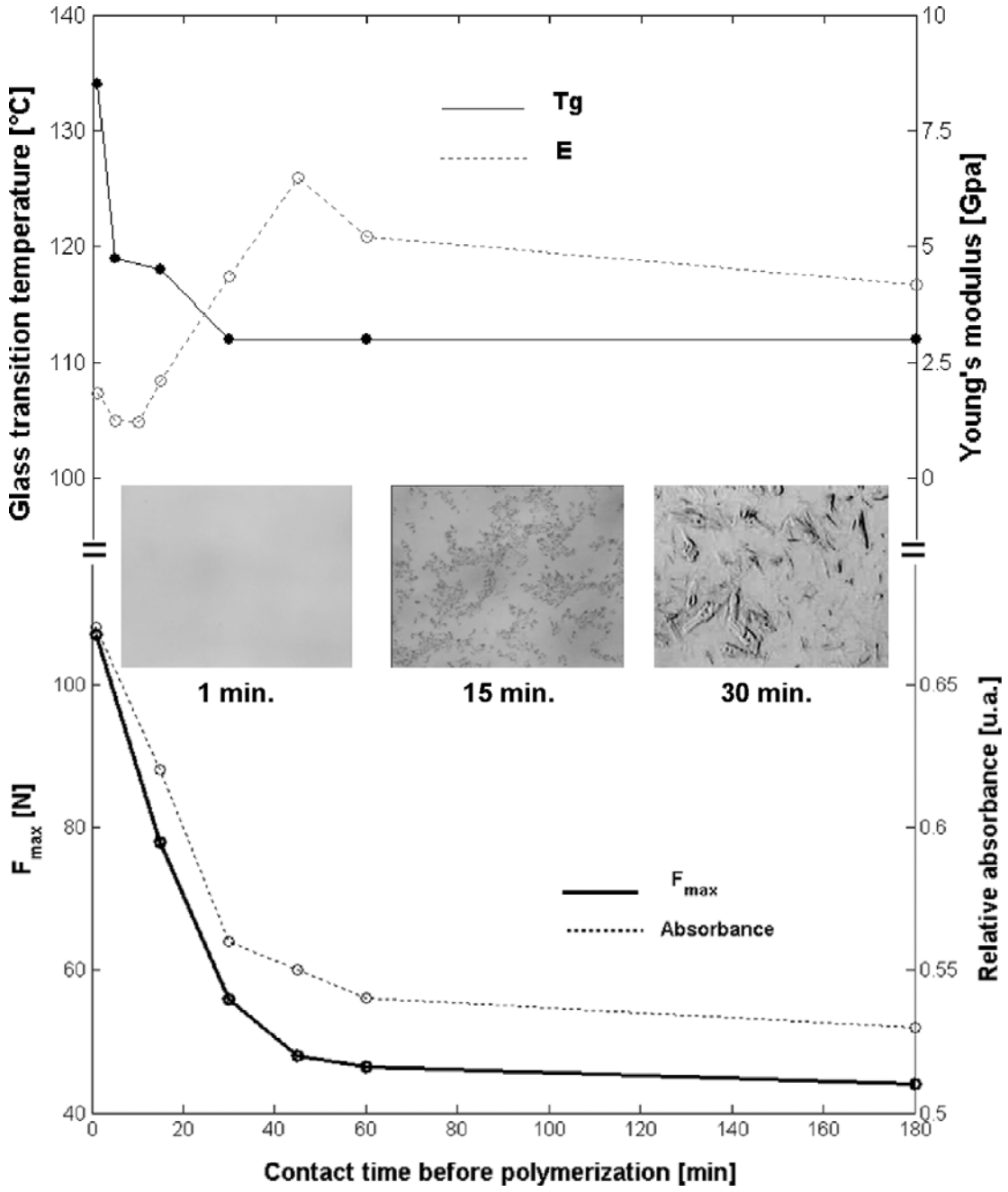

FIGURE 5 Variation of the ultimate load (F_{max}) using a three-point flexure test, the OH group relative absorbance obtained from FTIR, the glass transition temperature obtained from DSC and the Young's modulus obtained from a three-point flexure test as a function of contact time between the DGEBA-IPDA mixture and the degreased aluminum substrate before starting curing cycle (i).

flexure test with a 150-μm thick coating) as a function of the contact time between the DGEBA-IPDA liquid mixture and the degreased aluminium substrate before starting the curing cycle (ii). The practical

adhesion considerably decreases during the first 60 min and remains relatively constant for longer times. The same trend is observed for the relative absorbance of OH groups and the glass transition temperature. On the contrary, the Young's modulus increases during the first 30 min and remains constant thereafter. Moreover, in Figure 5 we have reported optical microscopy photographs of the IPDA monomer after application onto degreased aluminum as a function of time. The crystal size increases during the first 30 min and remains constant thereafter. This means that it is possible to control the interphase formation by limiting the contact duration between the liquid prepolymers and metallic substrates. That can be easily achieved. Thus, right after the application of the DGEBA-IPDA mixtures onto treated metallic substrates (less than 2 min) panels were immediately introduced in a oven at 190°C and kept in for 6 hours before cooling down. This curing cycle is referred to as (ii). In Table 2 we report the final physical and mechanical properties of both bulk polymers and films according to the two different curing cycles (i and ii) as a function of the aluminum surface treatment. We observe that bulk mechanical properties (E) are identical, irrespective of the curing cycle and the surface treatment. However, the bulk physical properties (Tg) are slightly different due certainly to a slight diamine evaporation during the (ii) curing cycle. For the 30-μm thin film on aluminium with the curing cycle (i) we observe, as explained previously, that the mechanical and physical properties are quite different from the bulk ones revealing the interphase formation irrespective of the surface treatment. However, for the 30-μm thin film on aluminium with the (ii) curing cycle mechanical and properties are the same as those of the bulk, irrespective of the surface treatment, indicating that the interphase was not formed or that the interphase is so thin that we are unable to observe it.

TABLE 2 Mechanical (E) and Physical (Tg) Properties of DGEBA-IPDA Systems

Material	Curing cycle	E [GPa]	Tg [°C]
30-μm coating on anodized Al	(i)	17	101
	(ii)	3.1	156
30-μm coating on chemically etched Al	(i)	14	104
	(ii)	3.1	154
30-μm coating on degreased Al	(i)	10	108
	(ii)	3.2	154
Bulk	(i)	3.2	163
	(ii)	3.1	156

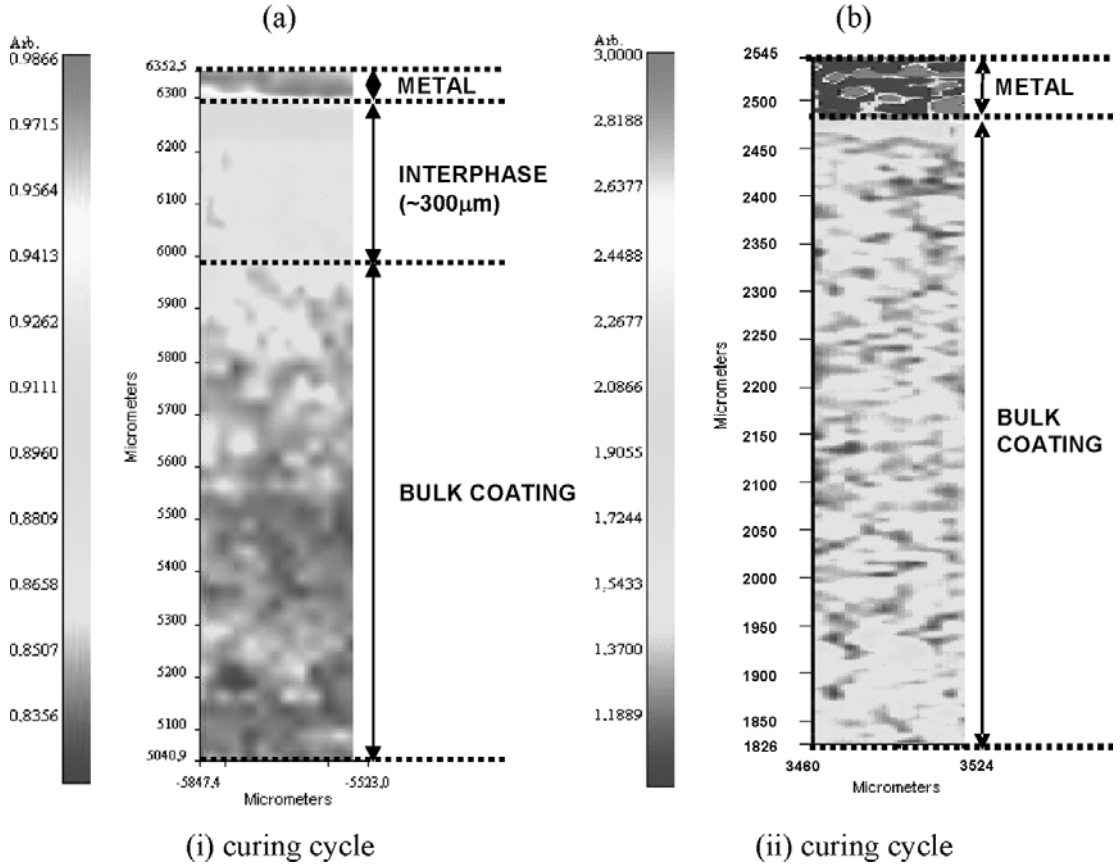

FIGURE 6 Micro-FTIR map (normalized amine band intensity) of DGEBA-IPDA block polymer applied onto chemically etched aluminum after (a) curing cycle (i) and (b) curing cycle (ii) (The top of the sample was initially in contact with the metal).

To check that the interphase formation mechanisms took place either in coatings or volumes a transmission infrared map was performed. The cured polymer stiffener was debonded during the three-point flexure test, so it was possible to slice (perpendicular to the surface of the adherent) and to analyze the epoxy-amine polymer block. Maps obtained on degreased aluminum are presented in Figure 6 (the top of the sample was initially in contact with the metal). In Figure 6a, curing cycle (i) was used and an interphase (corresponding to the region where band ratios vary), and a bulk region (with homogenous properties) are observed. The thickness of the interphase obtained is about 200–300 μm. On the contrary, in Figure 6b no interphase was observed when curing cycle (ii) is used.

The practical adhesion measurement being relevant to an adhesional failure (*i.e.*, within the interphase region), obviously, the interphase properties have to be considered.

In recent works we have reported that the consideration of the mechanical interphase properties is of prime importance to understand the mechanical behavior of bonded structures [32,33]. To point out the role of the interphase formation on the fracture toughness we used the model developed in order to calculate both residual stresses and the critical strain energy release rate. For tri-layer systems (*i.e.*, when curing cycle (i) was used) residual stresses were calculated using the Young's modulus gradient, within the interphase, observed experimentally [32]. Obviously, for bi-layer systems (*i.e.*, when curing cycle (ii) was used), residual stresses were calculated using the Young's modulus of the bulk coating. Figures 7 and 8 represent the profiles of residual stresses in the tri and bi-layer systems, respectively.

The maximum stresses within the tri-layer system were at the interphase/metal interface while the ones observed in the bi-layer system were at the bulk coating/metal interface irrespective of the surface treatments. Moreover, we can observe, for tri-layer systems (*i.e.*, which contain an interphase), an increase of the maximum stress intensity compared with the bi-layer systems (*i.e.*, without interphase). Thus the presence of the interphase may favor an increase

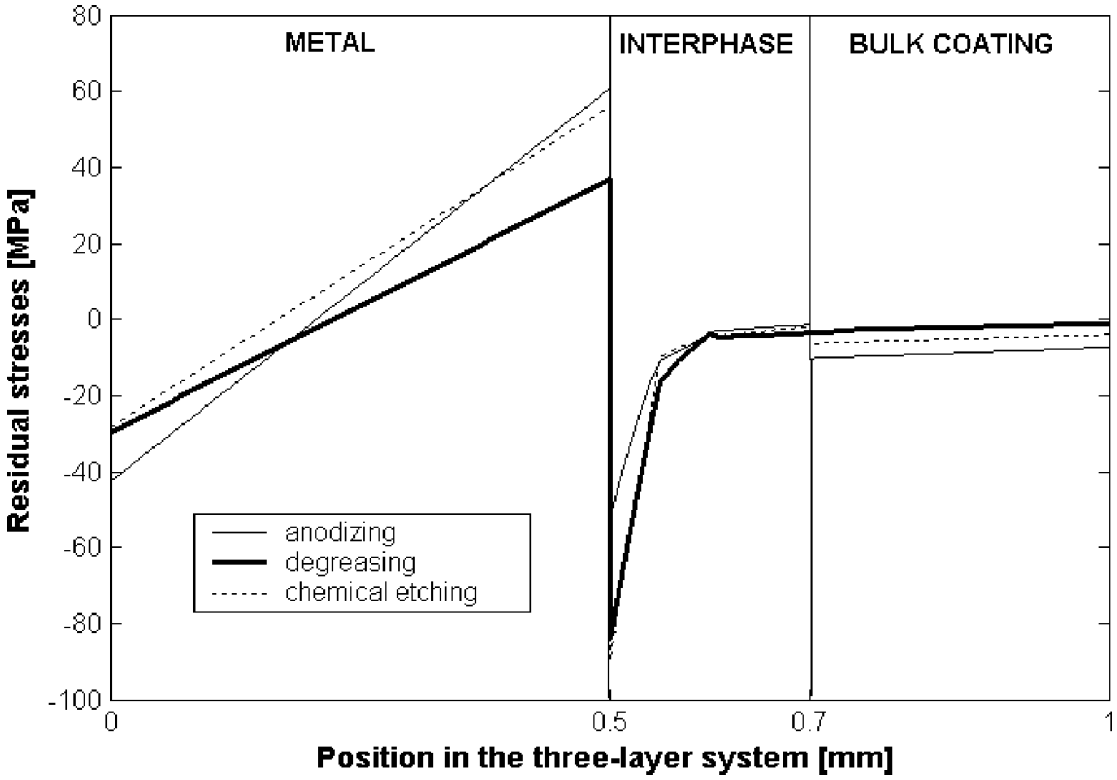

FIGURE 7 Profile of residual stresses in the trilayer system (curing cycle [i]).

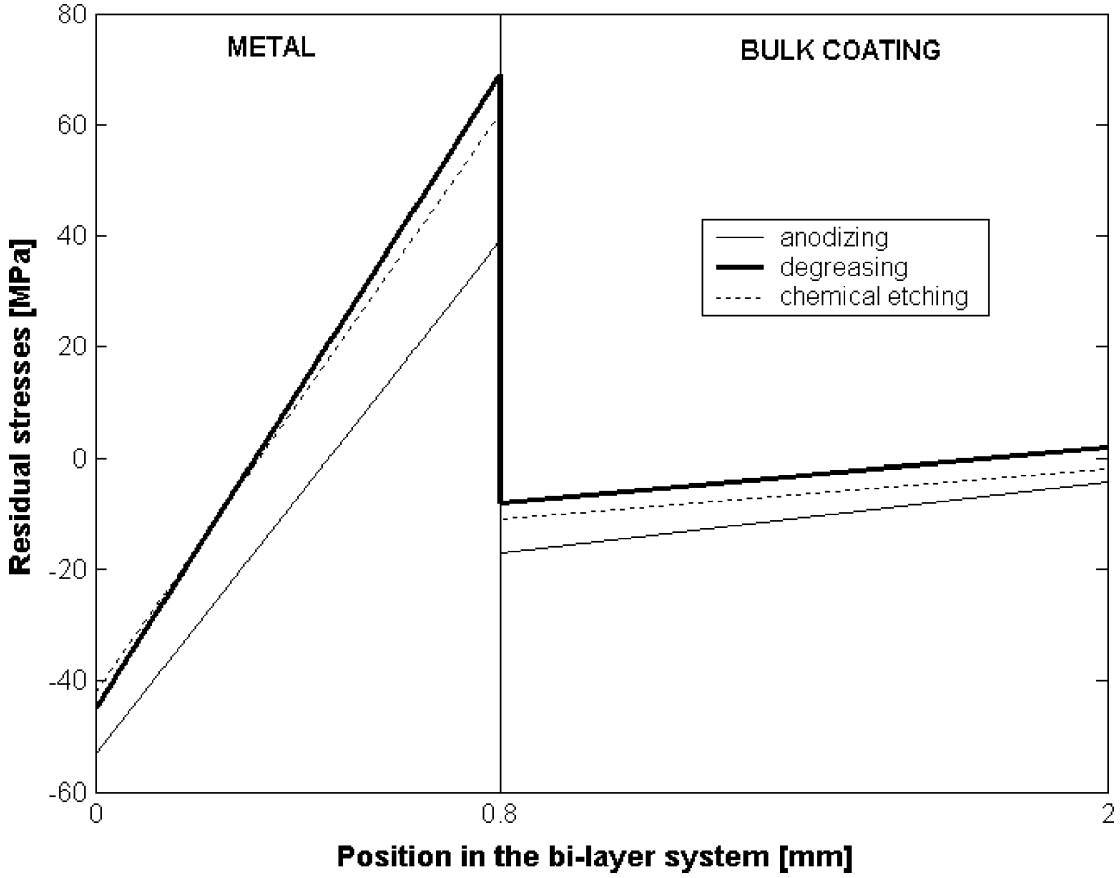

FIGURE 8 Profile of residual stresses in the bilayer system (curing cycle [ii]).

of the residual stresses. From those results we can assume that the practical adhesion will decrease as soon as the interphase will be formed. By using the model previously developed we have calculated the quantity of energy required to initiate the failure using Equation (7). From the experimentally obtained maximum load and by using the residual stress profile determined for chemically etched, degreased and anodized aluminum with (curing cycle [i]) or without (curing cycle [ii]) interphase we have determined the critical strain energy release rate (see Figure 9). The formation of the interphase leads to a fracture toughness decrease. This may be due to the increase of residual stresses during the interphase formation (probably induced by the presence of crystals) as suggested in Figure 5. Moreover, when residual stresses are considered, the surface treatments do not play a significant role in fracture toughness. Indeed, we have shown that the residual stresses depend on the surface treatment [32], but, when they are considered in the critical strain energy release rate calculation, the fracture toughness seems to be independent of the surface treatment. The overall results show that to correlate the work of adhesion to

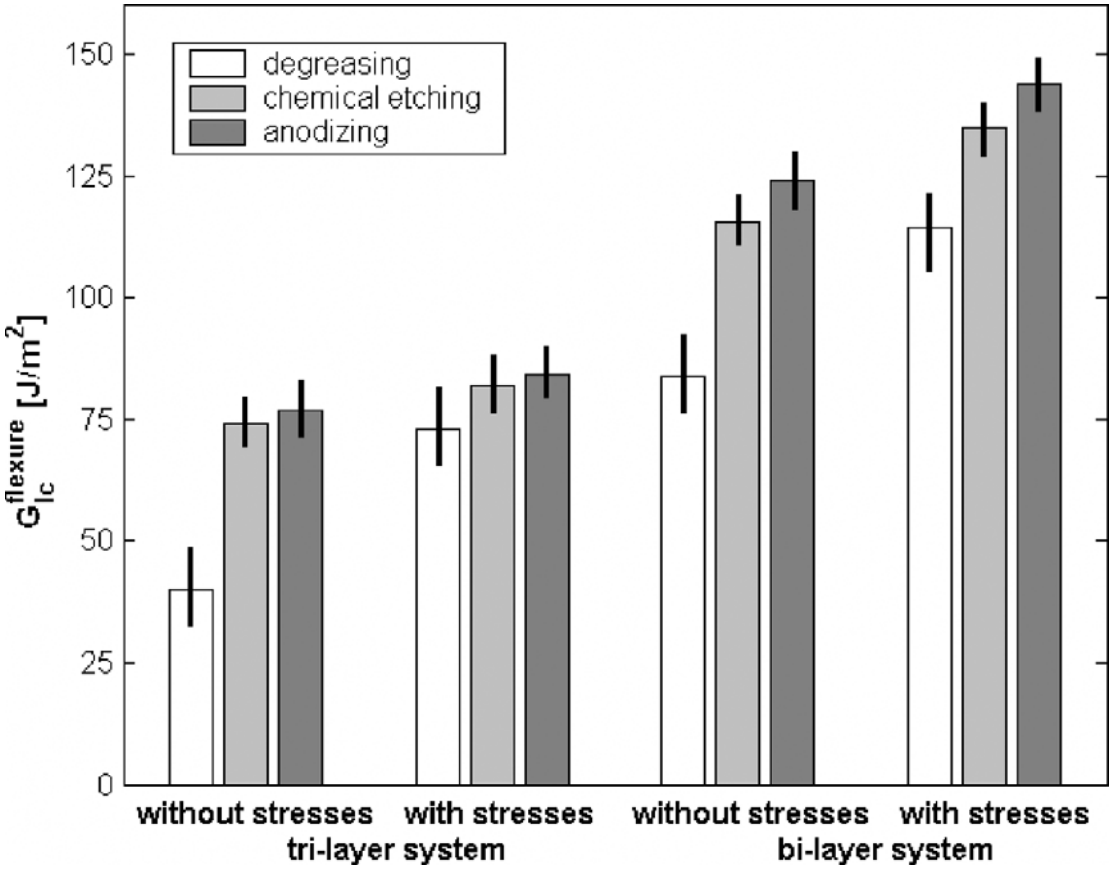

FIGURE 9 $G_{Ic}^{flexure}$ results obtained by using the model for degreased, chemically etched, and anodized aluminum for either a bilayer system (curing cycle [ii]) or a trilayer system (curing cycle [i]) with or without residual stresses.

practical adhesion it is of prime importance to have an intrinsic parameter. Mechanical properties of the interphase such as Young's modulus gradient and also residual stress profile have to be considered.

CONCLUSIONS

When epoxy-diamine prepolymers are applied onto metallic substrates, interphases between the coating part having the bulk properties and the metallic surface are created. The mechanisms of the interphase formation are dominated by dissolution and diffusion phenomena. Because dissolution and diffusion phenomena were observed the interphase formation should be related to the liquid-solid contact duration between liquid prepolymers and metallic substrates. By using an appropriate curing cycle for prepolymers it is possible to control the interphase formation. We observed that the interphase formation decreases the practical adhesion by increasing residual stresses. Thus, we have clearly shown that the practical adhesion

represented here by the critical strain energy release rate, depends on the residual stresses. Samples that contain an interphase are subjected to a higher residual stress level compared with the ones without interphase. However, the presence of the interphase and, more particularly, the organo-metallic complexes (chelate) certainly seem to be responsible for the increase of the residual stresses. When a tri-layer system with residual stresses is considered, the fracture toughness seems to be independent of the surface treatment. Obviously, to characterize practical adhesion using ultimate parameters such as ultimate load before failure and/or assuming a perfect interface between the organic coating and the substrate is not sufficient and/or or useful in order to correlate practical adhesion to fundamental adhesion. For otherwise identical systems overall properties of coatings, including those of the interphase, depend on the contact duration between metallic surfaces and liquid prepolymers and can explain the different findings observed in the literature.

REFERENCES

[1] Fauquet, C., *Ph.D. thesis*, "Etude Expérimentale d'Une Interface ModèLe Aluminium/Adhésif Epoxy" (Université Paris 6, France, 1992).
[2] Walker, P., *J. Coating. Technol.* **52**, 49–56 (1980).
[3] Guminski, R. D. and Meredith, F. M. P., *J. Oil. Colour Chem. Assoc.* **44**, 93–98 (1961).
[4] Hine, P. J., Muddarris, S. E. L., and Packham, D. E., *J Adhesion Sci. Technol.* **1**, 69–78 (1987).
[5] March, J., Minel, L., Barthes-Labrousse, M. G., and gorse, D., *Appl. Surface Sci.* **133**, 270–286 (1998).
[6] Crompton, G. S., *J. Mater. Sci.* **24**, 1575–1581 (1989).
[7] Kim, Y. H., Walker, G. F., Kim, J., and Park, J., *J. Adhesion Sci. Technol.* **1**, 331–339 (1987).
[8] Allara, D. I. and White, C. W., *Amer. Chem. Soc.* 273–284 (1978).
[9] Von Preissing, F. J., *J. Appl. Phys.* **66**, 4262–4628 (1989).
[10] Nairn, J. A., *Int. J. Adhesion Adhesives* **20**, 59–70 (2000).
[11] Guo, S., Dillard, D. A., and Nairn, J. A., *Int. J. Adhesion Adhesives* **26**, 285–294 (2006).
[12] Scafidi, P. and Ignat, M., *J. Adhesion Sci. Technol.* **12**, 1219–1242 (1998).
[13] Orsini, H. and Schmit, F., *J. Adhesion* **43**, 55–68 (1993).
[14] Thouless, M. D. and Jensen, H. M., *J. Adhesion Sci. Technol.* **8**, 579–586 (1994).
[15] Mulville, D. R. and Vaishnav, R. N., *J. Adhesion* **7**, 215–233 (1975).
[16] Mittal, K. L., in *Adhesion Measurement of Thin Films, Thick Films and Bulk Coatings*, K. L. Mittal (Ed.) (ASTM, Philadelphia, 1978), pp. 5–17.
[17] Sharpe, L. H., *J. Adhesion* **4**, 51 (1972).
[18] Safavi-Ardebili, V., Sinclair, A. N., and Spelt, J. K., *J. Adhesion* **62**, 93–111 (1997).
[19] Finlayson, M. F. and Shah, B. A., *J. Adhesion Sci. Technol.* **5**, 431–441 (1990).
[20] Anderson, G. P. and DeVries, K. L., in *Treatise on Adhesion and Adhesives* R. L. Patrick (Ed.) (Marcel Dekker, New York, 1989), Vol. 6.

[21] Brewis, D. M. and Critchlow, G. W., *Int. J. Adhesion Adhesives* **17**, 33–38 (1997).
[22] Schön, J., Nyman, T., Blom, A., and Ansell, H., *Composites Science Technol.* **60**, 173–184 (2000).
[23] Todo, M., Jar, P.-Y. B., and Takahashi, K., *Composites Science Technol.* **60**, 263–272 (2000).
[24] Williams, J. G. *Fracture Mechanics of Polymers* (Ellis Horwood, Chichester, UK 1980).
[25] Scott, J. M. and Phillips, D. C., *J. Mater.Sci.* **10**, 551–562 (1975).
[26] Reyes, G. and Cantwell, W. J., *Composites Science Technol.* **60**, 1085–1094 (2000).
[27] Schuecker, C. and Davidson, B. D., *Composites Science Technol.* **60**, 2137–2146 (2000).
[28] Bouchet, J. and Roche, A. A., *J. Adhesion* **78**, 799–830 (2002).
[29] Roche, A. A., Bouchet, J., and Bentadjine, S., *Int. J. Adhesion Adhesives* **22**, 431–441 (2002).
[30] Bentadjine, S., Roche, A. A., and Bouchet, J., in *Adhesion Aspects of Thin Films*, K. L. Mittal (Ed.) (VSP, Utrecht, The Netherlands 2001), Vol. 1.
[31] Bouchet, J., Roche, A. A., and Hamelin, P., *Thin Solid Films* **355–356**, 270–276 (1999).
[32] Bouchet, J., Roche, A. A., and Jacquelin, E., *J. Adhesion Sci. Technol.* **15**, 321–343 (2001).
[33] Bouchet, J., Roche, A. A., and Jacquelin, E., *J. Adhesion Sci. Technol.* **15**, 345–369 (2001).
[34] Bouchet, J., Roche, A. A., and Jacquelin, E., and Scherer, G. W., in *Adhesion Aspects of Thin Films*, K. L. Mittal (Ed.) (VSP, Utrecht, The Netherlands 2001), Vol. 1.
[35] Roche, A. A., Dole, P., and Bouzziri, M., *J. Adhesion Sci. Technol.* **8**, 587–609 (1994).
[36] DeNogarro, F. F., Guerrero, P., Corcuera, M. A., and Mondragon, I., *J. Appl. Polym. Sci.* **56**, 177–192 (1995).
[37] Roche, A. A., Gaillard, F., Romand, M. J., and VonFahnestock, M., *J. Adhesion Sci.-Technol.* **1**, 145–157 (1987).
[38] Roche, A. A., Dumas, J., Quinson, J. F., and Romand, M., in *Mechanics and Mechanisms of Damage in Composites and Multi-materials*, D. Baptiste (Ed.) (Mechanical Engineering Publications, London, 1991).
[39] Roche, A. A., Behme, A. K., and Solomon, J. S., *Int. J. Adhesion Adhesives* **2**, 249–253 (1982).
[40] Rives, B., *Ph.D. thesis*, "Adhérence de Primaires Aéronautiques sur Oxydes d'Aluminium" Université Paul Sabatier Toulouse III, France, 1999.
[41] Aufray, M. and Roche, A. A., in *Adhesion-Current Research and Applications*, W. Possart (Ed.) (Wiley-VCH, Verlag, 2005).